Hindawi
Advances in Civil Engineering
Volume 2023, Article ID 8864328, 15 pages
https://doi.org/10.1155/2023/8864328

Research Article

Dam Breach Modeling and Downstream Flood Inundation Mapping Using HEC-RAS Model on the Proposed Gumara Dam, Ethiopia

Manamno Beza,[1] **Amdeselassie Fikre**,[2] **and Alene Moshe**[1]

[1]*Department of Hydraulic and Water Resources Engineering, Wolaita Sodo University, Sodo, Ethiopia*
[2]*Department of Hydraulic and Water Resources Engineering, Debre Tabor University, Debre Tabor, Ethiopia*

Correspondence should be addressed to Manamno Beza; manabeza06@gmail.com

Received 24 August 2023; Revised 3 October 2023; Accepted 14 October 2023; Published 10 November 2023

Academic Editor: Valeria Vignali

This study was, therefore, taken up to dam breach modeling and downstream flood inundation mapping. To achieve this objective, the software ArcGIS Version 10.4 extension program of HEC-GeoRAS Version 10 tool was used for HEC-RAS model development, to generate modeling reach and floodplain cross-sectional geometric data and for downstream inundation mapping and HEC-RAS Version 6.3.1 tool was used for subject dam break simulation and unsteady flood routing at downstream regions. Von Thun and Gillette regression equation was selected to estimate the breach parameter and the result shows that breach bottom width is 113 m, side slope 0.5H : 1V and breach development time is 0.85 hr for overtopping and bottom width is 111 m, and side slope 0.5H : 1V and breach development time is 0.83 hr for pipping. During analysis of flood routing the peak discharge at the dam site is 19,753.68 m^3/s occurred at 4 hr for overtopping and 25,128.1 m^3/s at time to peak 4 hr for pipping.

1. Introduction

Dams and waterway impoundments help the public by storing water for flood control, recreation, drinking water, the production of hydroelectric power, stormwater management, the construction of wildlife habitats, and irrigation. Despite the dam's advantage, flooding caused by it poses a risk that could destroy all natural, private, and public property [1]. According to Alabi et al. [2], the history of water retention structures used for various purposes coexists with the history of those structures' failures. In both extreme weather events and regular times, dam failures can happen for a number of reasons, such as seepage, overtopping, and structural collapse [3].

A dam can be breach due to various reasons, including natural disasters such as heavy rainfall, earthquakes, or landslides, or due to human-made factors such as poor maintenance, design flaws, or construction errors [4–6]. In some cases, a combination of factors can lead to the failure of a dam. For example, heavy rainfall can cause water levels to rise rapidly, leading to increased pressure on the dam structure. If the dam is not designed or maintained to withstand such pressures, there is a risk of failure. Another common cause of dam failure is the presence of defects or weaknesses in the dam structure. These defects can arise due to poor construction practices, inadequate materials, or lack of maintenance over time [7, 8]. Over time, these defects can cause the dam to weaken and eventually fail, leading to catastrophic consequences downstream.

Water-impounding structures are called "provided that include powerful energy" in the law of world humanitarian due to the potential impact of possible devastating on the life that are found in the ecosystem [9]. Dam failures are very infrequent, but when they do happen, they can result in tremendous damage and fatalities. There have been an average of almost 10 dam failures between 1848 and 2017, according to McCann's [10] and Wahl's [11] research on U.S. dam failures. Since many dams have failed in the past in various parts of the world and caused catastrophic harm to human lives, property, and the environment in general [12, 13–15] taking good care of their safety is thus a crucial issue when setting up and implementing dams. At all times,

the risks associated with the storage of water must be controlled to decrease the likelihood of failure. Design engineers and dam owners are inherently liable for the potential serious consequences of dam failures [16].

Predicting the outflow hydrograph of the reservoir and routing it at d/s valley to evaluate its effects of the probable dam failure are the two main activities in the analysis of a dam a failure [17, 18]. It is crucial to correctly forecast the breach outflow hydrograph and its timing in relation to events in the failure process that could prompt the beginning of evacuation efforts when people at danger are situated close to a dam [18]. A similar study by Mhmood et al. [19] presents a study on the potential consequences of a hypothetical failure of the Haditha Dam in Iraq using HEC-RAS. The study uses a numerical model to simulate the flood wave that would result from such a failure and analyzes the potential impact on downstream areas. The results show that a dam failure would cause significant damage to infrastructure, agriculture, and residential areas, and that emergency preparedness plans should be put in place to mitigate the potential impact.

At the time of failure of the dam, modeling is necessary to evaluate the flood hydrograph of the discharge resulting from the dam breach due to the propagation of flood waves and their period of occurrence [6, 20]. Infrastructure like roads, railways, bridges, and buildings may be completely destroyed by the impact of such a wave in developed areas. If there is no opportunity for early warning and evacuation, dam failure may result a massive loss of life [20]. Large amounts of sediment and debris are also moved during such significant flooding, and there is also a chance that any nearby mines or chemical plants will release contaminants into the environment which are affected by the flood [20, 21].

Due to their suitability for any type of foundation, simplicity of construction, and relative affordability due to the use of locally accessible materials, earthen dams are one of the types of dams that are widely used throughout the world, including Ethiopia [17, 22, 23]. However, it is prone to failure despite being appropriate and cost-effective [1, 24, 25].

Gumara earthen dam irrigation project is one of the identified irrigation projects in South Gondar administrative zone. It is a strong project to be constructed on the river Sendega. Gumara comprises of 33.0 m high earth fill dam with a central clay core on river for impounding inflows of the river during the monsoon period. The River Gumara has a total catchment area of 385 km^2 at the proposed dam site [26]. The catchment area extends over the following four weredas: Farta, Iste, Fogera, and Dera. The weir is located about 28 km downstream of dam site and hence the catchment area at weir site is 1,189 km^2, which is largely cultivated and highly exposed to severe erosion hazard [26].

Therefore, the purpose of the research was to model the breach at proposed Gumara embankment dam. Two failure mode was considered one is due to overtopping of the flow over the dam and piping of the dam.

The significance of doing this includes for safety assessment: It helps in assessing the potential risks associated with dam breaches, which is crucial for ensuring the safety of communities living downstream. Emergency preparedness can develop effective emergency response plans and evacuation strategies to minimize the impact of such events. Infrastructure design: The research can inform the design and construction of dams by providing insights into the behavior of dams during breach scenarios, helping engineers improve their structural integrity. Environmental impact: Understanding dam breaches can help evaluate the environmental consequences, such as downstream flooding, allowing for better management and mitigation strategies. Risk management: The research aids in quantifying the probability and magnitude of dam breaches, enabling policymakers and stakeholders to make informed decisions regarding risk reduction measures and insurance policies.

Overall, this study contributes to enhancing dam safety, emergency preparedness, infrastructure design, environmental sustainability, and risk management in the field of water resources engineering.

2. Materials and Methods

2.1. Description of the Study Area. Gumara watershed, which is one of the watersheds of the Tana sub-basin. The geographical location of the Gumera watershed is found between 11° 34′ 41.41″ N and 11° 56′ 36.95″ N latitude to 37° 29′ 30.48″ E and 38° 10′ 58.01″ E longitude (Figure 1).

Gumara River is one of the main streams on the east side, flowing into Lake Tana. The river flows generally in a westerly direction for a length of 132.50 km till Lake Tana. The catchment area from the head to Tana is 1,893 km^2. The subbasin of Gumara includes mainstream Gumara and its substreams such as Kinti, Sendega, and Meteray. From which, the proposed Gumara irrigation dam will be constructed at Sendega river, which has a total catchment area of 385 km^2 at the dam site [26].

The Gumara watershed is characterized by diverse topographic conditions. The upper part of the watershed is characterized by mountainous and highly separated terrain with steep slopes and the downstream part is a gentle slope with elevation ranges from 3,702 m in the mountainous area to 1,785 m in the flood plain near to the Lake Tana (Figure 1) [27].

The rainfall distribution is unimodal in nature and 85% of the total annual rainfall occurs from June to September. The mean monthly rainfall distribution ranges from 1,204.66 to 1,504.09 mm. The monthly mean maximum temperature fluctuates from 34°C in October to more than 29°C in April and minimum temperature fluctuates from 4.8°C in October and December to 9.8°C in May [28, 29].

2.2. Data Collection

2.2.1. Materials and Software Used. The software HEC-GeoRAS Version 10 which is the extension of ArcGIS Version 10.4 was used for the development of HEC-RAS model, to extract modeling reach and floodplain cross-sectional geometric data and for downstream inundation mapping. Global Mapper Version 13 with Google Earth was used to assess and edit study area map and for remote sensing of the

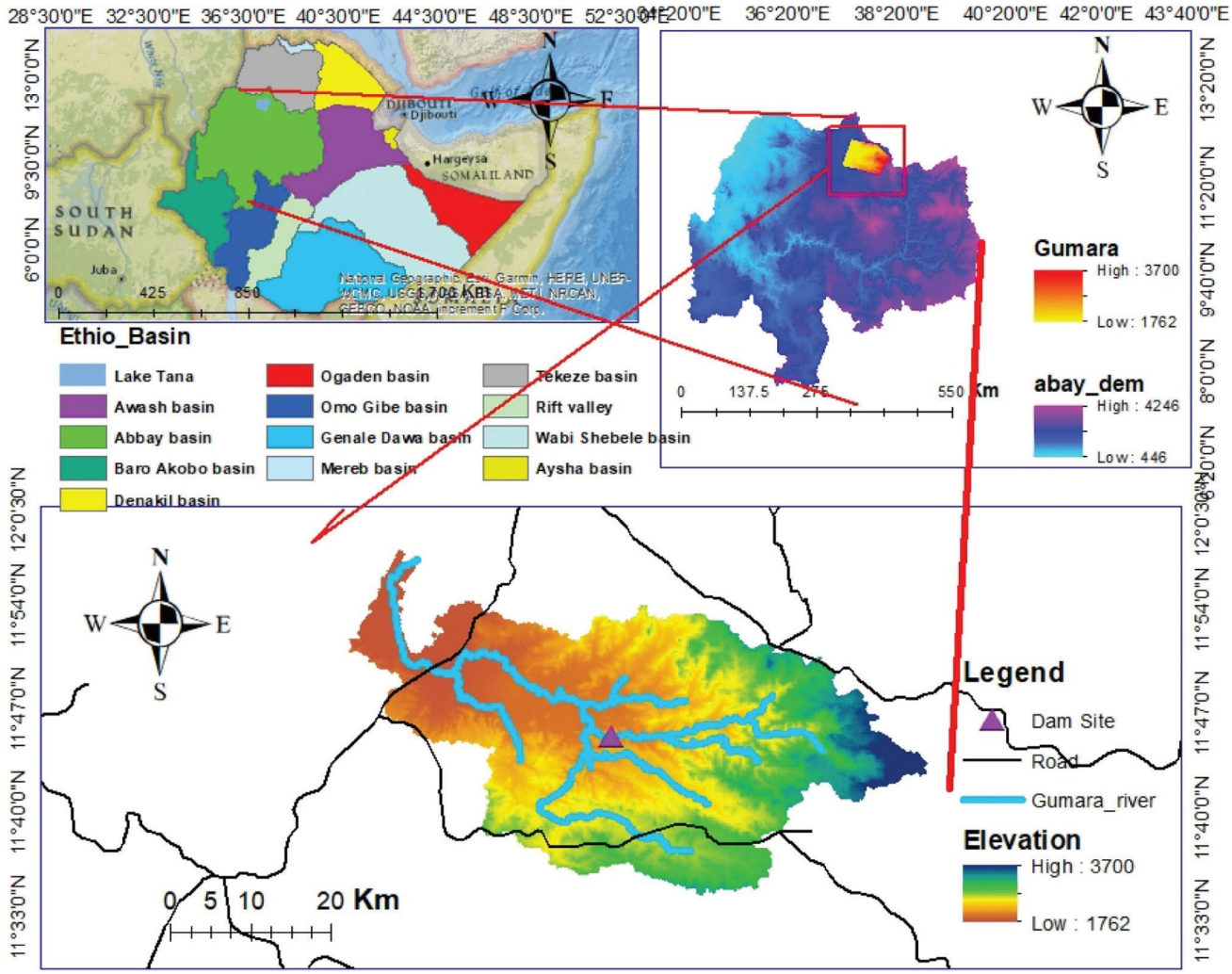

Figure 1: Study area.

developed structures like water structures, cities, and recent land use/land cover. HEC-RAS Version 6.3.1 model was used for dam break estimation and routing at downstream side of the dam. Also, the output of the model was processed using statistical programs.

2.2.2. Data Types and Sources. The prerequest for breach modeling is the quality of the data during the estimate of the effect of the failure to obtain a correct result. Some crucial data were collected to model dam breach and to determine the effects of dam failure on the downstream flood plain. The primary and secondary data were collected for the study area from different sources and field observations.

(*1*) *Hydrological Data*. Data such as inflow hydrograph, probable maximum flood (PMF), reservoir capacity, and flood frequency analysis input for hydraulic modeling in this research were obtained from the hydrological and reservoir capacity analysis of the design document of Gumara irrigation dam [26].

(*2*) *Probable Maximum Flood*. The PMF as shown below (at dam site) (Figure 2) which is obtained in the design document of the Gumara dam from hydrological part.

(*3*) *Spatial Data*. A 20 m × 20 m digital elevation model (DEM) was obtained from the United States Geological Survey website (https://www.usgs.earthexplorer). It is used to extract the river channel, left and right banks, and each cross-section used for the analysis of Gumara irrigation dam breach in triangulated irregular network (TIN). It was done using ArcGIS with the extension tool HEC-GeoRAS along the river up to 28 km downstream of the dam.

(*4*) *Dam and Spillway Characteristics*. To achieve the objective of this study, the general dam profiles data were taken from the design document and project completion report [26]. It includes dam type, dam size, location of the dam, elevation of the downstream toe of dam, design water storage pool elevation, maximum flood surcharge elevation, spillway crest elevation, crest of dam elevation, and height of the dam (Table 1).

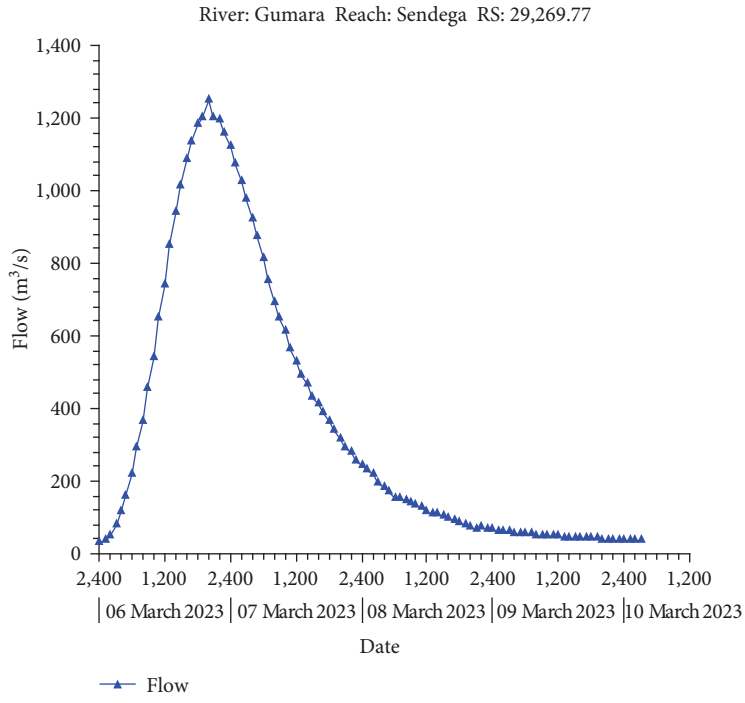

Figure 2: Probable maximum flood.

Table 1: Silent features of proposed Gumara dam.

Features	Properties
Type of dam	Earth fill with central impervious core
Height of dam	33 m
Dam crest width	10 m
Dam crest elevation	1,933 m
Length of dam at crest	505.3 m
U/s slope	3H : 1V
D/S slope	2.5H : 1V

2.3. Breach Parameter Estimation. The analysis of dam breach, estimating the breach station, size, and time are necessary to obtain a real value of the outflow hydrograph and downstream flooding. HEC-RAS model needs the modeler to insert mid-line location of the breach in the dam (location), failure mode (overtopping or piping), size (bottom elevation, bottom width, left and right-side slope (H : V), critical breach development time, and weir or pipe coefficient.

2.3.1. Failure Location. The type and shape of the structure, type and mode of failure and the driving force of the failure are a major element to estimate the location of the failure. For this study, the failure is at center of the dam and expands equal in both directions.

2.3.2. Failure Mode. Even though, HEC-RAS hydraulic models are including only piping and overtopping failure type, the other mode of failures is included by either of the two methods. Failure mode is the mechanism for starting and growing breach. In this case, the type of failure includes overtopping and piping type. Overtopping failure begins at the top of dam and grow but piping failure mode can start at any elevation/location and expand till it reaches to the maximum.

2.3.3. Breach Shape. The breach shape resulting from dam overtopping during a dam break can vary and includes rectangular, triangular, and trapezoidal shapes. However, trapezoidal shapes are commonly observed in research studies on breach formations [1, 8, 14, 15, 30–32]. Therefore, trapezoidal shape is selected for this study. Trapezoidal shape of the dam breach consists height of the breach, breach width, and side slope in H : V.

Various regression equations can be found in different literature related to dam safety studies. These equations are utilized to calculate breach parameters, including breach width and breach development time [33–35]. For this study, a comparison was made between various methods to determine the breach parameters for both overtopping and piping methods. The parameters in question were the breach width and the critical breach development time.

2.3.4. Breach Weir Coefficient. The user needs to input the weir coefficient in the HEC-RAS model, which directly impacts the magnitude of the peak outflow hydrograph for a given breach. Estimating this coefficient requires an understanding of the failure process. Generally, during overtopping failure of an earthen dam, head cut erosion begins downstream of the dam embankment. Dams with larger storage volumes are likely to fail down to the natural stream bed elevation during the breach widening phase, resulting in a peak outflow. In such cases, a weir coefficient typical of a broad crested weir with a long crest length ($C = 2.6$) is

Table 2: Dam breach weir and piping coefficients.

Dam type	Overflow/weir coefficients	Piping/pressure flow coefficient
Earthen clay/clay core	2.6–3.3	0.5–0.6
Earthen sand and gravel	2.6–3.0	0.5–0.6
Concrete arch	3.1–3.3	0.5–0.6
Concrete gravity	2.6–3	0.5–0.6

recommended. However, for dams with relatively low water volume compared to the dam height, the peak flow may occur while the breach is still cutting through the dam. In these situations, a weir coefficient typical of a sharp crested weir ($C = 3.2$) is more suitable. In piping failure breaches, the flow rate through the dam is modeled using an orifice pressure flow equation. The recommended values for the piping/pressure flow coefficients are range from 0.5 to 0.6. Guidelines for selecting breach weir and piping flow coefficients are provided in Table 2.

Considering the medium storage capacity of the Gumara embankment dam [26] in relation to its height, a weir coefficient of 2.6 has been chosen for overtopping, while a weir coefficient of 0.5 has been selected for piping.

2.4. Equations Used to Predict Breach Parameter. In dam breach analysis, determining breach parameters is crucial. These parameters can be divided into two categories: geometric parameters and hydrographic parameters [35]. Dam breach parameters define the development of geometric parameters of breach depth (h_b), height of water (h_w), top breach width (B_t), average breach width (B_{ave}), bottom breach width (W_b), and breach side slope factor (Z). There are different empirical equations which are used to estimate the breach parameters. Among this, the most widely used methods are USBR [36], Lawrence Von Thun and Gillette [35], Froehlich [37], and MacDonald and Langridge-Monopolis [34]. Here, in this study, all the four methods are applied and compared with each other to determine which breach parameter estimation method is suitable to estimate the breach parameter [38].

2.4.1. USBR (1988) [36]. According to USBR [36], breach width (B) and failure time (t_f) are given as follows:

$$\text{Breach width}, B(\text{m}) = 3 \times h_w, \tag{1}$$

$$\text{Failure time}, t_f(\text{hr}) = 0.011 \times B, \tag{2}$$

where h_w is the height measured from the initial reservoir water level to the breach bottom elevation, which is assumed to be the streambed elevation at the toe of the dam.

2.4.2. MacDonald and Langridge-Monopolis (1984) [34]. They estimated the quantity of eroded embankment materials (Ver) (m^3) for earth and rock dams as follows:

$$\text{Ver} = 0.0261 \times (V_{out} \times h_w)^{0.769}, \text{for earth fill dam}, \tag{3}$$

Table 3: Values of C_b are based on reservoir size.

Capacity of reservoir (mm^3)	C_b (m)
<1.23	6.3
1.23–6.17	18.3
6.17–12.3	42.7
>12.3	54.9

$$\text{Ver} = 0.00348 \times (V_{out} \times h_w)^{0.852}, \text{for rock fill dam}, \tag{4}$$

$$t_f(\text{hr}) = 0.00348 \times (\text{Ver})^{0.364}, \tag{5}$$

$$W_b(\text{m}) = \frac{\text{Ver} - h_b^2(CZ_b + h_b Z_b Z^3/3)}{h_b\left(C + \frac{h_b Z_3}{2}\right)}, \tag{6}$$

where V_{out} is the volume of water discharged through breach (m^3), h_w is the hydraulic depth of water at dam at failure above breach bottom (m), C is the crest width, Z is the u/s slope dam, Z_2 is the d/s slope of dam, $Z_3 = Z_1 + Z_2$, and $Z_b = 0.5$.

MacDonald and Langridge-Monopolis stated that the breach should be trapezoidal with side slopes of 0.5H : 1V.

2.4.3. Lawrence Von Thun and Gillette (1990) [35]. The equations suggested by Lawrence Von Thun and Gillette [35] for the average breach width and failure time are given by:

$$B(\text{m}) = 2.5 \times h_w + C_b, \tag{7}$$

$$t_f(\text{hr}) = 0.015 \times h_w, \text{ for highly erodible dam}, \tag{8}$$

$$t_f(\text{hr}) = 0.0209 \times h_w, \text{ for erosion resistance dam}, \tag{9}$$

where h_w (m) is the depth of water at the dam at the time of failure and C_b is the function of reservoir capacity and is given in Table 3.

Von Thun and Gillette suggested using breach side slopes of 1H : 1V for earthen dams with a clay core.

2.4.4. Froehlich (1995) [37]. Froehlich has defined the average breach width, side slope, and the time of failure as follows:

$$B_{ave}(\text{m}) = 0.1803 \times \text{Ko} \times V_w^{0.32} \times h_b^{0.19}, \tag{10}$$

$$t_f(\text{hr}) = 0.00254 \times V_w^{0.53} \times h_b^{-0.9}, \tag{11}$$

where Ko = 1.4, for overtopping failure and Ko = 1, for piping failure, h_b (m) is the height of breach, and V_w (m^3) is the volume of breached water. Froehlich further suggested breach side slopes of 1.4 : 1 (horizontal : vertical) for piping and 1 : 1 for overtopping.

2.4.5. Froehlich (2008) [33]. In 2008, Dr. Froehlich updated his breach equations based on the addition of new data Dr.

Froehlich utilized 74 earthen, zoned earthen, and earthen with a core wall (i.e., clay), and rock fill date sets to develop as set of equations to predict average breach width, side slopes, and failure time. The data that Froehlich used for his regression analysis had the following ranges:

(i) Height of the dams: 3.05–92.96 m.

(ii) Volume of water at breach time: $0.0139–660.0 \times 10^6\,m^3$.

Froehlich's regression equations for average breach width and failure time are as follows:

$$B_{av} = 0.27\mathrm{Ko}V_w{}^{0.32}h_b^{0.04}, \quad (12)$$

$$t_f = 63.2\sqrt{\frac{V_w}{gh_b^2}}, \quad (13)$$

where B_{ave} is the average breach width (m), Ko is constant (1.3 for overtopping failures, 1.0 for piping), V_w is the reservoir volume at time of failure (cubic meters), h_b is the height of the final breach (meters), g is the gravitational, and t_f = breach formation time (seconds).

Froehlich's [33] paper suggested breach side slopes of 1 : 1 (horizontal : vertical) for piping and 0.7 : 1 for overtopping.

2.5. Hydraulic Model Development. This section provides a detailed discussion of the dam breach analysis model, which involves predicting the dam breach hydrograph and routing it downstream at critical locations. The analysis was conducted using hydraulic modeling with HEC-RAS. Additionally, ArcMap software was utilized for all related tasks, and HEC-GeoRAS served as the interface between GIS and the hydraulic modeling. The Environmental System Research Institute ArcMap software Version 10.4 was used in this study for ArcGIS. ArcMap is the primary component of ArcGIS, a geospatial processing software. HEC-GeoRAS was used to create inundation depth maps and visualize hydraulic modeling results.

2.5.1. HEC-GeoRAS Development. HEC-GeoRAS comprises a set of tools that are tailor made to process geospatial data in order to facilitate the development of hydraulic models and the analysis of water surface profile results [39]. In this study, HEC-GeoRAS, a tool compatible with ArcMap, is utilized to generate RAS layers in ArcGIS. These RAS layers are then used to extract crucial information required for hydraulic modeling (HEC-RAS). This study employed HEC-GeoRAS to extract elevation data from DEMs in the TIN format and create several layers, including the stream centerline layer, bank lines layer, flow path layer, and cross-sectional cut line layer (Table 4). After creating these RAS layers, HEC-GeoRAS tools and menus were utilized to assign and populate attribute data. Once all attributes were completed, the data were written out to the HEC-RAS geospatial data exchange format and imported into the HEC-RAS hydraulic model.

Table 4: Component of HEC-GeoRAS layers with its description [39].

RAS layer	Description
River center line	Is employed to determine the connectivity of the river network and allocate river stations to computation points
X-sectional cut lines	Used to extract elevation transects from the DEM at specified locations and other cross-sectional properties
Bank lines	Used in conjunction with the cut lines to identify the main channel from overbank areas
Flow path center lines	Used to identify the center mass of flow in the main channel and overbanks to compute the downstream reach lengths between cross-sections
Land use	Used to assign flow roughness factors (Manning's n values) to the cross-sections
Ineffective flow areas	Used to identify the location of nonconveyance area
Blocked obstructions	Used to identify obstructions to flow
Bridges	Used to extract the top of road data from the DEM at specified locations
Inline structures	Used to extract the weir profile from the DEM for inline structures in this study the inline structure is dam
Lateral structures	Used to extract the weir profile from the DEM for structures the pass flow perpendicular from the main channel
Storage areas	Used to define the extent of detention areas and develop the elevation volume relationship from the DEM
Storage area connections	Used to extract the weir profile from the DEM for connections between storage areas

(*1*) *Roughness Values.* Determining Manning's roughness coefficient (or Manning's n) is crucial for modeling open channel flows. However, directly determining this coefficient is nearly impossible when studying natural river flows, including unsteady channel network flows.

Determining the roughness coefficient (n) in natural channels is challenging to accomplish in the field. The article presented several factors that impact the values of roughness coefficients [40]. The friction slope is a crucial parameter that requires careful selection. The study identified several major land cover types, including moderately cultivated, dense woodland, intensively cultivated land, wooded grassland, open woodland, natural forest cover, natural forest with coffee, coffee farm with shade trees, riverine forest, bamboo forest, plantation forest, settlement, shrub land, and open grassland. As a result of these land cover types, the Manning roughness value of the channel varies along the flow direction from one point to another.

2.6. Floodplain Mapping. This section analyzes the aerial extent of flooding downstream area for Gumara irrigation dam breach analysis. Two failure mode scenarios were used, namely overtopping and piping modes of failure. The study considers the reservoir conditions, including normal pool (spillway crest level) and maximum storage elevation (top of the dam crest) for the downstream consequence of Gumara irrigation dam breach.

After completing the dam breach simulation in HEC-RAS, the results were exported to ArcGIS and stored for the next inundation delineation process. The ArcGIS tool HEC-GoeRAS extension and RAS Mapper automatically delineate flood plains or inundation as a postprocessing function of HEC-RAS.

To map the floodplain downstream of Gumara irrigation dam, water surface elevations on the cross-section cut lines were used within the limits of the bounding polygon. A polygon refers to a TIN layer in ArcGIS that defines a zone that connects the outer points of the bounding polygons.

2.6.1. HEC-RAS Development. This study utilized HEC-RAS modeling, which was developed by the U.S. Army Corps of Engineers' Hydrologic Engineering Centre Version 6.3.1. The software has a graphical user interface and can perform 1D steady- and unsteady-flow simulations. It also has the capability to model dam breach events under various scenarios. HEC-GeoRAS and ArcGIS were used to extract cross-sections, stream centerlines, and other geometric features of the stream from GIS data.

The study analyzed dam failure scenarios for sunny day or nonhydrologic and hydrologic events to evaluate the impact of a dam breach on downstream populations and property damage. HEC-RAS 6.3.1 was used to model overtopping and piping failure breaches for earthen dams, and the resulting flood wave was routed downstream using unsteady flow equations. When GIS data (terrain data) are available, HEC-GeoRAS can be used to map the resulting flood inundation.

(*1*) *External Boundary Condition*. External boundary condition (EBC) refers to the most upstream and downstream ends of the river system, and it can have either an inflowing or outflowing river reach connected to the node. It includes inflow hydrographs, stage hydrographs, rating curves, or normal depth.

For Gumara irrigation dam breach analysis, there were two EBCs: upstream and downstream boundary conditions. Discharge hydrographs are typically input as upstream boundary conditions for unsteady flow models. In this study, the input hydrographs were a PMF flood event. The downstream boundary condition for Gumara irrigation dam was set at normal depth slope (percent slope) and downstream of the flood in which the flood entered to large gorge.

(*2*) *Internal Boundary Condition*. Internal boundary condition refers to the conditions at internal nodes where two or more reaches meet. These nodes serve as connections between river reaches with different roughness or bed slopes or where canal expansion occurs. They are denoted as junction boundary conditions and do not have hydraulic structures.

(*3*) *Initial Condition*. In the case of initial conditions, the actual parameter values of the river can affect the peak flood hydrograph that develops after a breach. Therefore, these parameter values should be entered as initial conditions in the HEC-RAS model at the beginning of the unsteady flow simulation. For Gumara irrigation dam breach analysis, the initial flow condition of the river system was considered, as there was an initial flow designed as excess flow over the spillway and allowable seepage analyzed by the dam owner.

Two initial conditions were entered in the HEC-RAS hydraulic modeling for unsteady flow analysis of Gumara irrigation dam breach: initial flow and initial elevation of water level in the reservoir at the time of starting a breach. The initial flow was estimated as the design capacity of the spillway since the dam breach was analyzed for the worst-case flood. The initial water level was taken as the elevation of maximum pool level.

3. Results and Discussion

In order to simulate a dam failure through the HEC-RAS environment, this requires a set of dam breaching parameters. The parameters needed for the HEC-RAS dam breach model are breach shape which is assumed as trapezoidal for this case, breach width, time to failure, and breach side slope. To conduct this analysis, information about reservoirs storage volume and height of water were provided for the reservoir in the study area.

3.1. Computation Time Step. Unsteady flow analysis was run for 1 day assuming an inflow magnitude equivalent to a base flow discharge that continues after the PMF inflow ends. One of the difficulties in unsteady flow model is model instability and numerical accuracy issues. These issues can get improved by selecting a time step; too large time step normally causes numerical diffusion and model instability, whereas too small-time step causes lengthy computational time and model instability as well. Thus, considering this, a 30 s computation interval was selected for the dam break analysis, and cross-sections were spaced at between 40 and 60 m intervals in reaches. When the river has steep slope and abrupt change the cross-section spacing is minimum, and in the case of flat slope, the spacing of the cross-section is increased.

3.2. Estimated Dam Breach Parameter. HEC-RAS software enables the modeling of breach development by entering key data and assumptions regarding the dam, the reservoir, and the breach characteristics. The breach parameters, such as breach formation time, bottom width of the breach, and breach side slope, are crucial in determining the related dam break peak outflow. Five methods have been defined to determine the breach parameters and related dam break peak outflow such as USBR, Macdonald, Von Thun, and Gillette [35] and Frohelic [33] done in HECRAS. The simulation for dam break model was done in breach plan data window in which the dam characteristics and dam breach parameters are entered.

Results of breach parameters show that Von Thun and Gillette equation gave the upper boundary of predicted

Table 5: Summary of breach parameter estimates in case of overtopping mode of failure.

Methods	Breach bottom width (m)	Breach failure time (hr)	Breach slope (H : 1V)
USBR	99	1.09	1
Von Thun and Gillette	113	0.85	0.5
MacDonald and Langridge-Monopolis	69	1.69	0.5
Froehlich [37]	105	1.44	1.4
Froehlich [33]	91	1.31	1

Table 6: Summary of breach parameter estimates in case of pipping mode of failure.

Methods	Breach bottom width (m)	Breach failure time (hr)	Breach slope (H : 1V)
USBR	99	1.09	1
Von Thun and Gillette	111	0.83	0.5
MacDonald and Langridge-Monopolis	71	1.67	0.5
Froehlich [37]	78	1.48	0.9
Froehlich [33]	73	1.35	0.7

values of the breach width (W_b) for overtopping cases of failure scenarios while lower values of W_b were given by MacDonald and Langridge-Monopolis. The predicted time of failure when using MacDonald and Langridge-Monopolis method gives the longest time required for breach formation for overtopping dam failure cases, while shortest values of t_f were given by Von Thun and Gillette (Table 5). The shorter time to peak is important for the necessary measures to be taken at downstream during failure case.

As shown in Table 5, Von Thun and Gillette and USBR equations tend to produce the smallest values, this might due to the sensitivity to dam depth (h_d) which is very small comparatively with the reservoir storage. Longest values of time of failure were given by MacDonald and Langridge-Monopolis.

Since, Gumara dam is an earthen embankment dam consisting of internal core zone and the amount of water which is stored behind the dam is huge, and the erosion progress is suddenly occurred, it can take short time to totally breach to its final width. Therefore, by comparing the five-regression equation result for both mode of failure, Von Thun and Gillette have minimum breach development time and selected for Gumara dam breach analyses in both mode of failure. For overtopping dam failure mode, the breach parameter estimated using Von Thun and Gillette the breach bottom width, breach failure time is 113 m and 0.85 hr. This shows that the breach has to grow 113 m wide in 0.85 hr (Table 6); so, the growth rate is 132.94 m/hr.

3.3. Breach Modeling in Overtopping Mode of Failure. In the case of overtopping mode of failure of the dam, the worst condition is when the reservoir behind the dam is full and peak of the most severe flood (PMF) impinges over the reservoir. The maximum discharge flows out from the breach dam are 19,753.68 (Figure 3) and 14,674.12 m^3/s (Figure 4) breach using Von Thun and Gillette and MacDonald and Langridge-Monopolis, respectively. Herein, when comparing the two methods to estimate the breach parameters in the cause of Von Thun and Gillette, the peak breach flow is greater than that is estimated by MacDonald and Langridge-Monopolis. Therefore, to reduce the downstream flood hazard and for preparedness considering the maximum peak breach is an indespensable task and thus Von Thun and Gillette method is considered for the remaining analysis of the breach.

Maximum flow, time to peak, and rate of flow and flood height of the breach of the dam at dam site are 5, 10, and 15 km, respectively, and distances below the Gumara dam are listed in the table below (Table 7). The results indicate that the peak stage is higher immediately downstream of the dam and decreases toward the downstream. It is observed that the maximum flood depth immediately on dam downstream location which is 5 km is 14.32 m and at 15 km is 10.23 m. The arrival times of peak flood at the dam and 15 km downstream of the dam are 4 and 12 hr, respectively, from the start of breach formation (Table 7).

Due to the change in cross-sectional area and slope, the velocity and flood height are varied but its peak values are decreased when goes to downward relative to the dam location ((Figure 5). The time to peak when analyzed by this method is found to be 4:00 hr from the initial flood beginning time 00 : 00, the dam breach and flood attenuation in the downstream regions has taken 24 hr. Also, due to the flat area of the watershed in the downstream side, the depth of the flood and velocity are reduced since the flood is dispersed in the flat area (Figure 5).

3.3.1. Routing of Flood Hydrograph for Overtopping. The two primary tasks in the hydraulic analysis of a dam breach are the prediction of the reservoir outflow hydrograph and the routing of that hydrograph through the downstream valley. The breach flood hydrograph is a plot of discharge versus time.

In the cause of overtopping mode of failure, the flood routing hydrograph was analyzed at different river station points, which are at dam site, 5, 10, and 15 km downstream

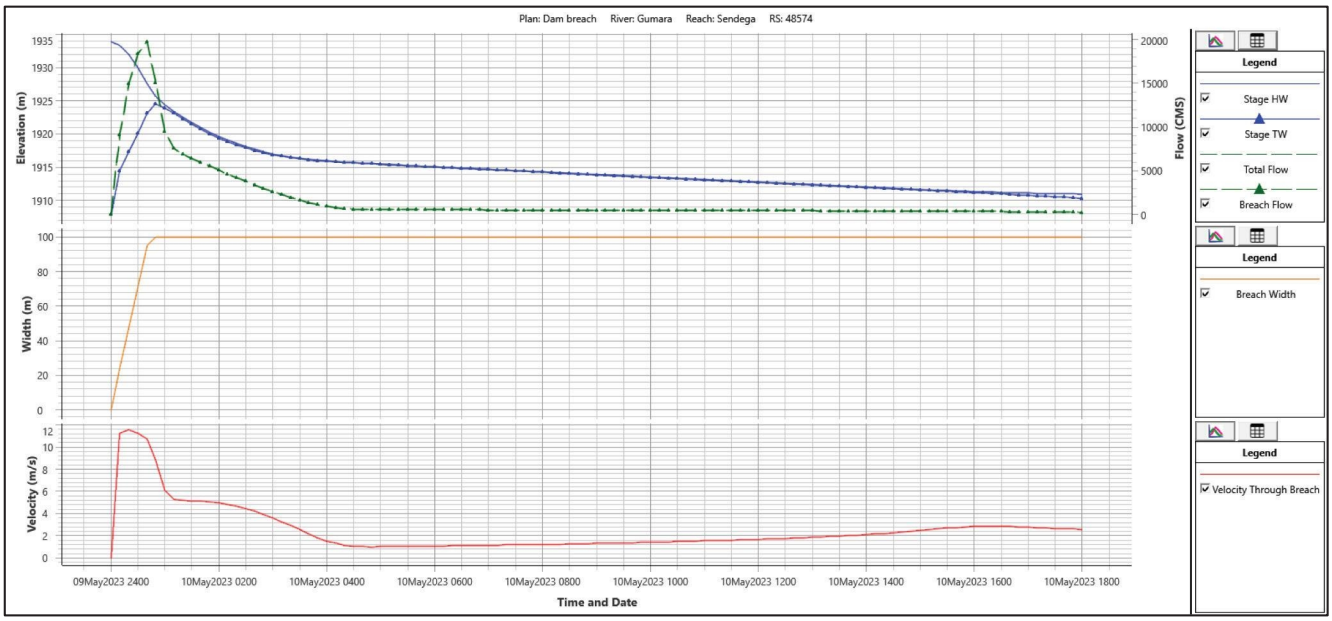

Figure 3: Breach hydrograph in case of overtopping using Von Thun and Gillette.

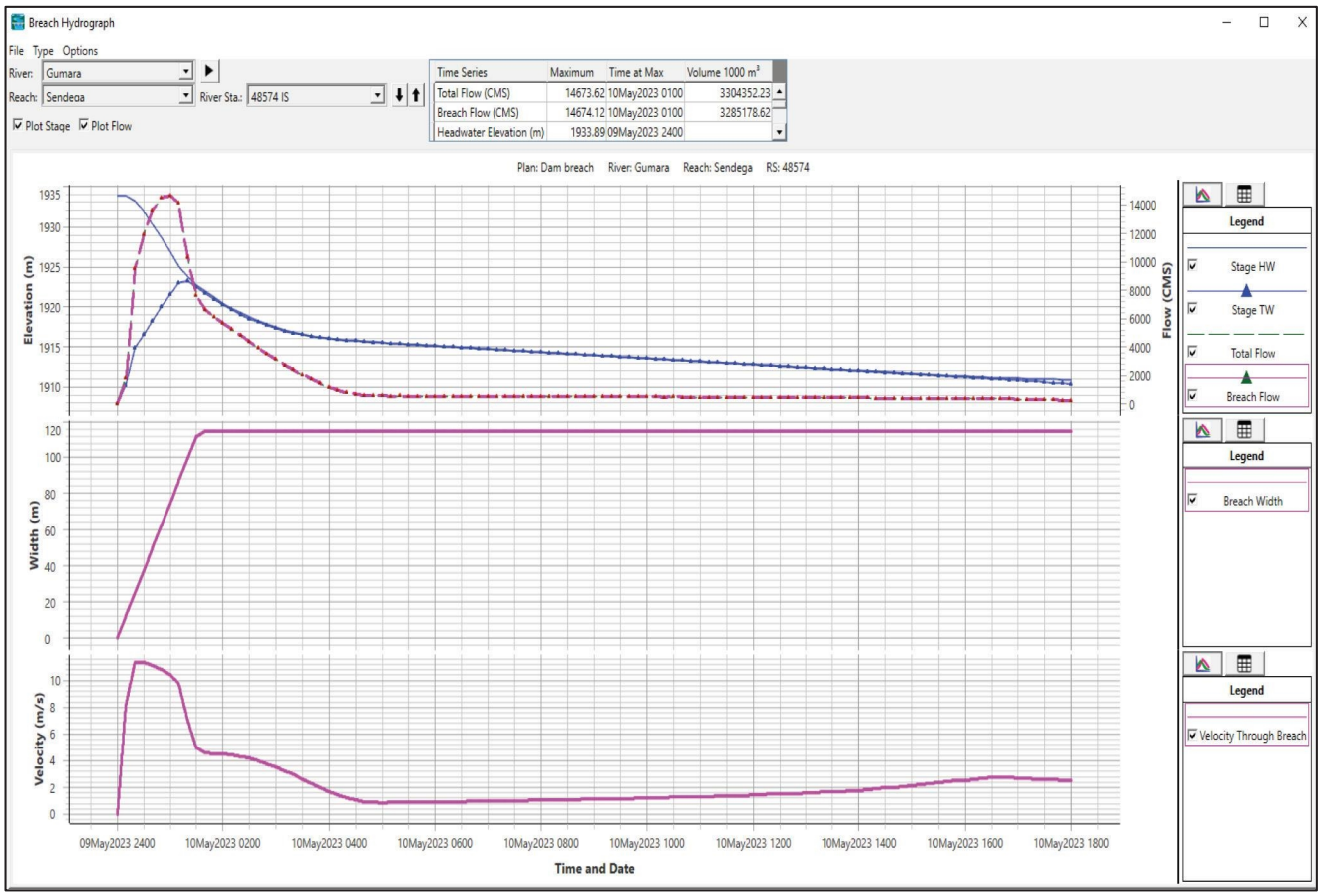

Figure 4: Breach hydrograph using MacDonald and Langridge-Monopolis.

Table 7: Maximum flow, time to peak, rate of flow, and flood height of the breach.

Chainage	Peak flow (m^3/s)	Velocity (m/s)	Flood height	Time to peak (hr)
At dam	19,753.68	11.54	15	4
5 km	17,253.68	10.54	14.32	6
10 km	15,159.95	9.75	12.57	9
15 km	12,705.96	5.03	10.23	12

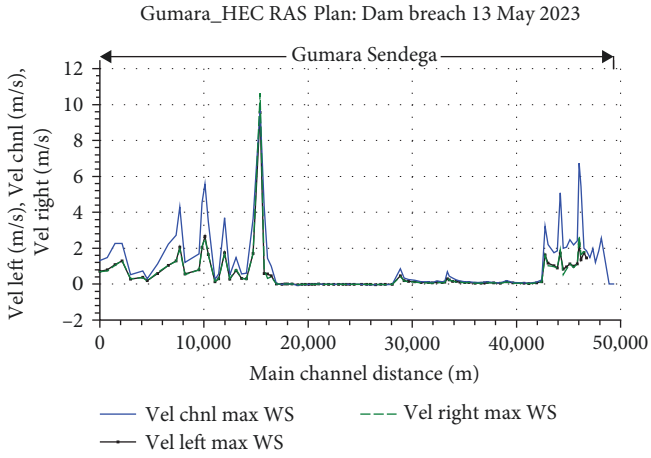

Figure 5: Right, left, and channel velocity.

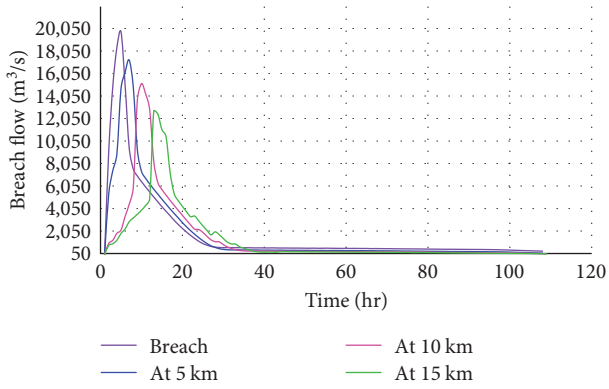

Figure 6: Routing of flood hydrograph d/s of the dam in overtopping mode of failure.

of the dam. Figure 6 shows the flood hydrograph for these different chainage points. The peak flood discharge at 5 km downstream of the dam is 17,253.68 m^3/s which is less than by 12.66% from the peak flood discharge coming out from the breach at dam site and it occur at after 2:00 hr at which the peak at the dam site occurred. At 10 km downstream location, the peak flood discharge is 15,159.95 m^3/s, which is less than by 23.25% and it is occurred after 5 : 00 hr at which the peak at dam site was occurred.

3.3.2. River Cross-Section at Different Chainage for Overtopping Mode of Failure. The cross-sections of river at upstream of the dam and downstream of the dam are 3.5, 6.32, and 8.53 km, shown in Figure 7, with its maximum water level during the breach of the dam.

3.4. Breach Modeling in Piping Mode of Failure. The most critical situation for piping mode of failure is at normal condition. The breach by piping depends on a sunny day condition rather than rainy day condition. As we stated under overtopping mode of failure, the breach parameters for piping mode of failure which is used as input for HEC-RAS model is calculated by Von Thun and Gillette regression equation. The water level of the reservoir when the dam breach started is 1,930 m and breach will continue up to bed level (Figure 8).

Similar to overtopping mode of failure, routing of flood hydrograph for piping mode of failure is analyzed at three chainage points which are 5, 10, and 15 km downstream of Gumara dam.

The maximum breach outflow and arrival time to peak breach outflow results obtained from HEC-RAS model simulation at dam for methods in case the of nonhydrologic (piping) breach scenario are given in Table 8.

For piping mode of failure, it is observed that the maximum flood depth immediately on dam downstream is 14.5 m, and 15 km downstream of the dam in the river reach considered is 11.23 m (Table 8). The arrival time of peak flood at the dam and 15 km downstream of the dam in the river reach is 4 and 13 hr, respectively, from the start of breach formation. The results indicate that the peak stage on the downstream region gradually decreases as the distance increases. At all the stations, the peak stage values are higher in pipping mode of failure than in overtopping mode of failure (Table 8).

3.5. Flood Inundation Mapping. The flood inundation mapping process plays a crucial role in assessing the impact of a dam breach and understanding the extent of flooding in downstream areas. In this case, the breach outflow hydrograph generated by the HEC-RAS model was utilized to delineate and map the flood inundation, including depth and velocity. The resulting maps (Figure 9(a)–9(c)) indicate valuable information on the flood depth, velocity distribution, and water surface elevation.

One of the key findings from the mapping exercise is the maximum flood depth of 15 m and a velocity of 15 m/s. Such high flood depths and velocities indicate the potential for severe damage of the dam and destruction in the affected areas. When comparing the design flood discharge and the peak flood which is obtaining in the result is very different, which makes the dam to fail in both mode of failures.

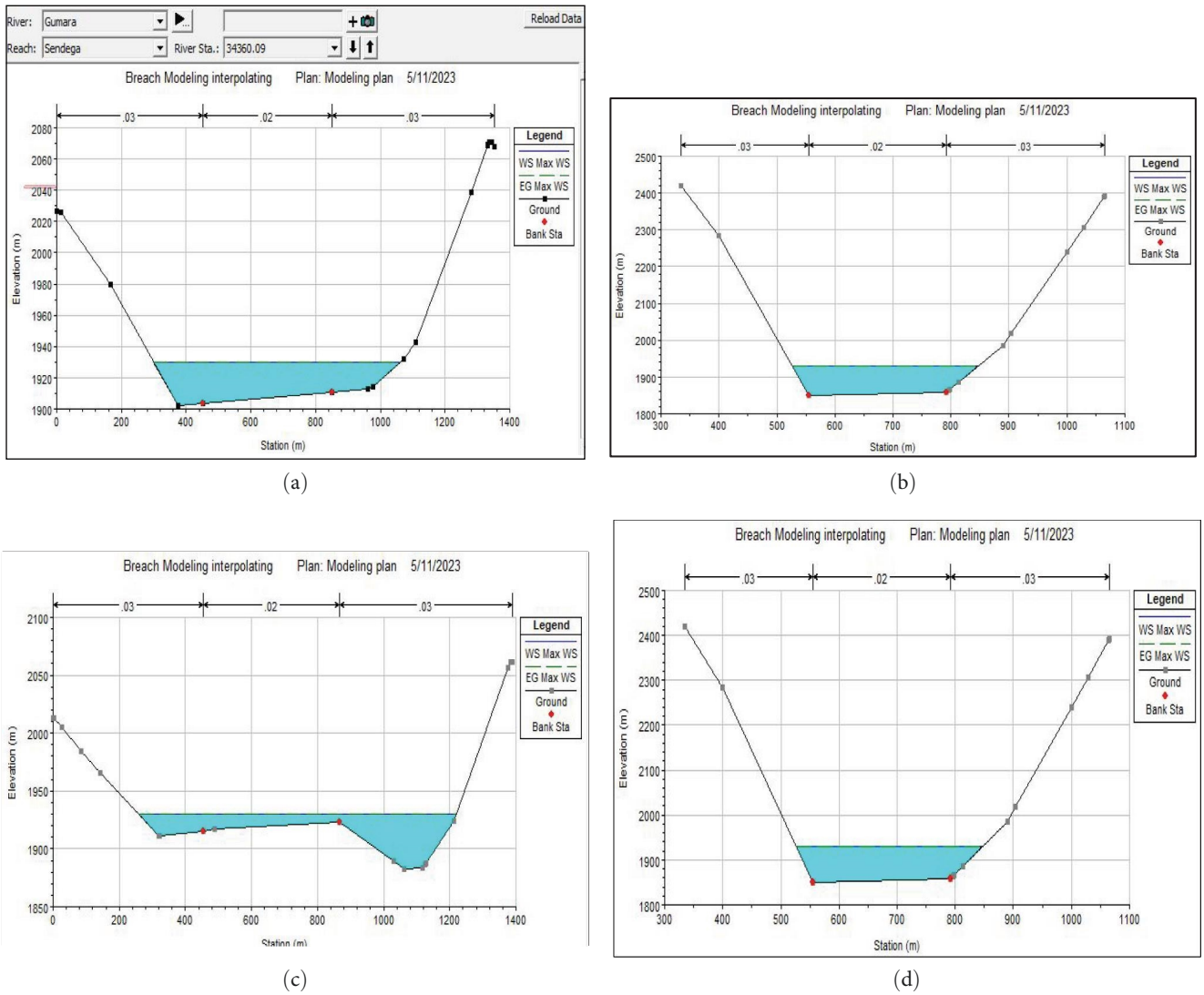

Figure 7: River cross-section at d/f chainage: (a) upstream of the dam, (b) 3.5 km downstream of the dam, (c) 6.32 km downstream of the dam, and (d) 8.53 km downstream of the dam.

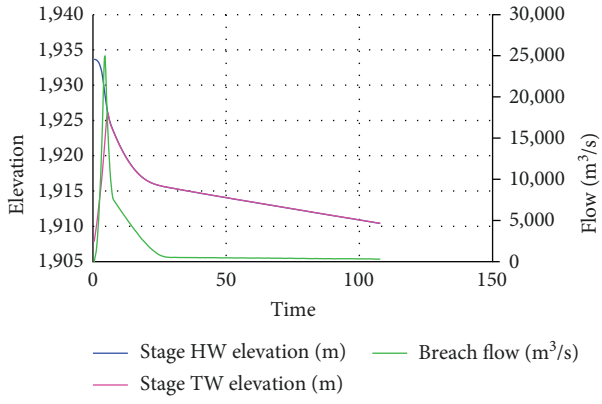

Figure 8: Breach hydrograph in case of pipping mode of failure.

Unfortunately, critical locations downstream have been significantly impacted by the flooding. On both sides of the river, there are traditional small-scale irrigation systems that have been inundated by the floodwaters. This poses a serious threat to the livelihoods of farmers who rely on these irrigation systems for their agricultural activities.

Furthermore, downstream of the dam, there are villages situated along the riverbanks. These villages are now completely affected by the floods resulting from the dam breach. The local population residing in these areas is facing immense challenges and hardships due to the destruction of homes, infrastructure, and disruption of essential services. The floodwaters have not only caused physical damage but have also posed risks to the safety and well-being of the affected communities.

In addition to the impact on traditional irrigation systems and villages, other areas have also been affected by the flooding. Approximately 28 km downstream of the dam, proposed irrigation land has been impacted on both sides of the river. This will have severe consequences for agricultural productivity and further exacerbate the challenges faced by farmers in the region. Moreover, the weirs constructed to

Table 8: Maximum flow, time to peak, rate of flow, and flood height of the breach for different chainage in case of pipping mode of failure.

Chainage	Peak flow (m^3/s)	Velocity (m/s)	Flood height	Time to peak (hr)
At dam	25,128.1	11.88	15	4
5 km	21,254.68	10.54	14.5	6
10 km	15,458.32	8.75	13.57	10
15 km	13,705.96	6.03	11.23	13

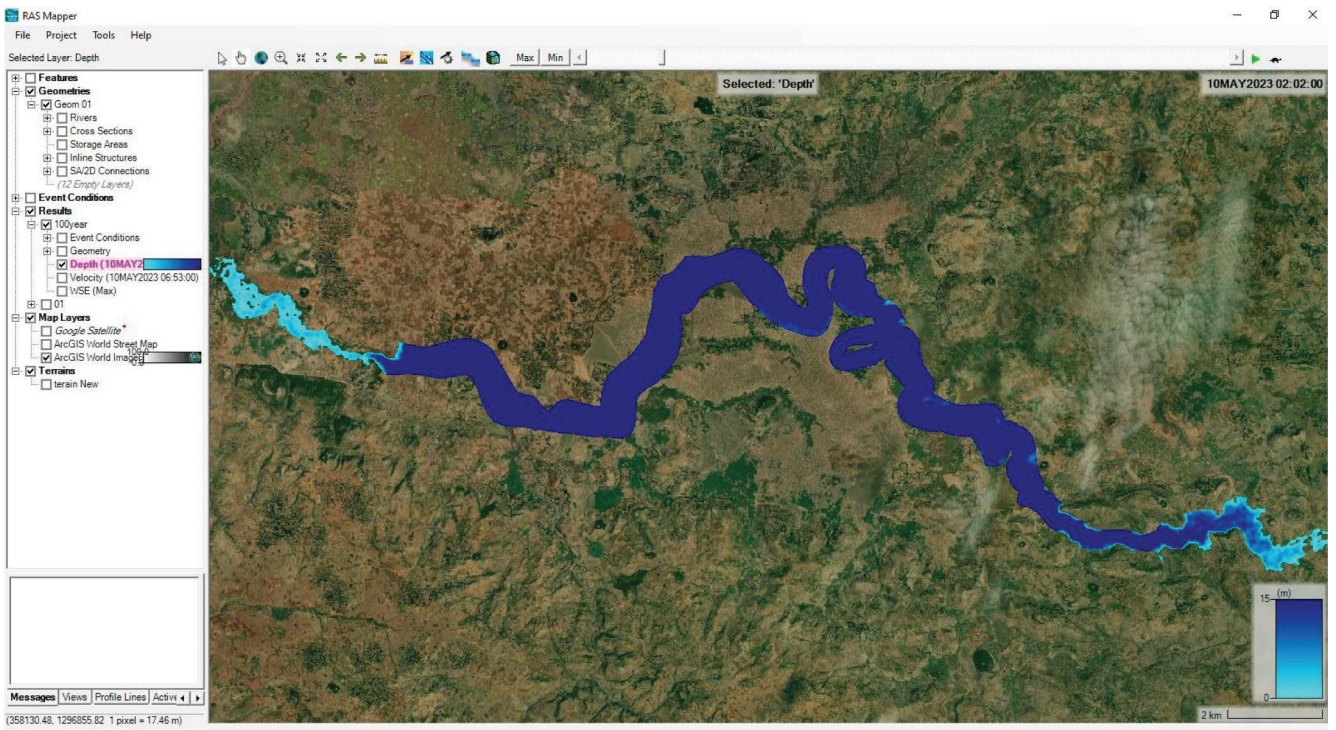

(a)

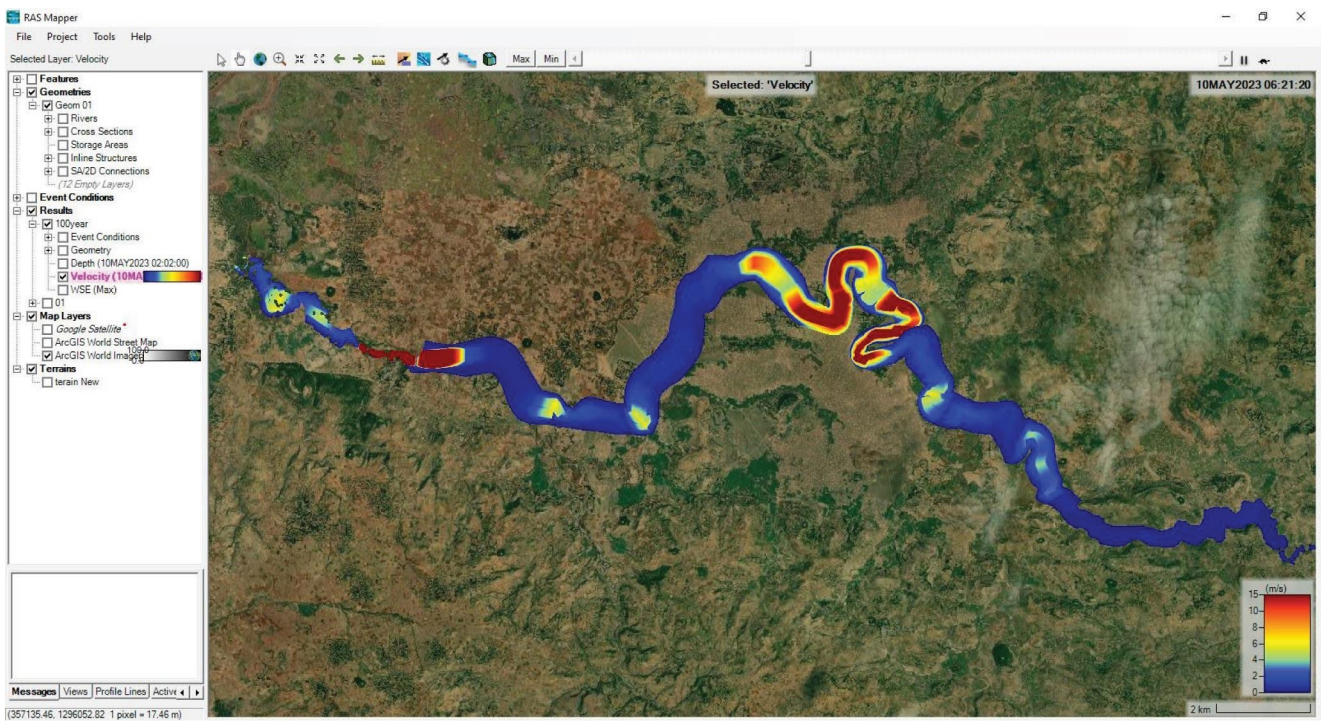

(b)

Figure 9: Continued.

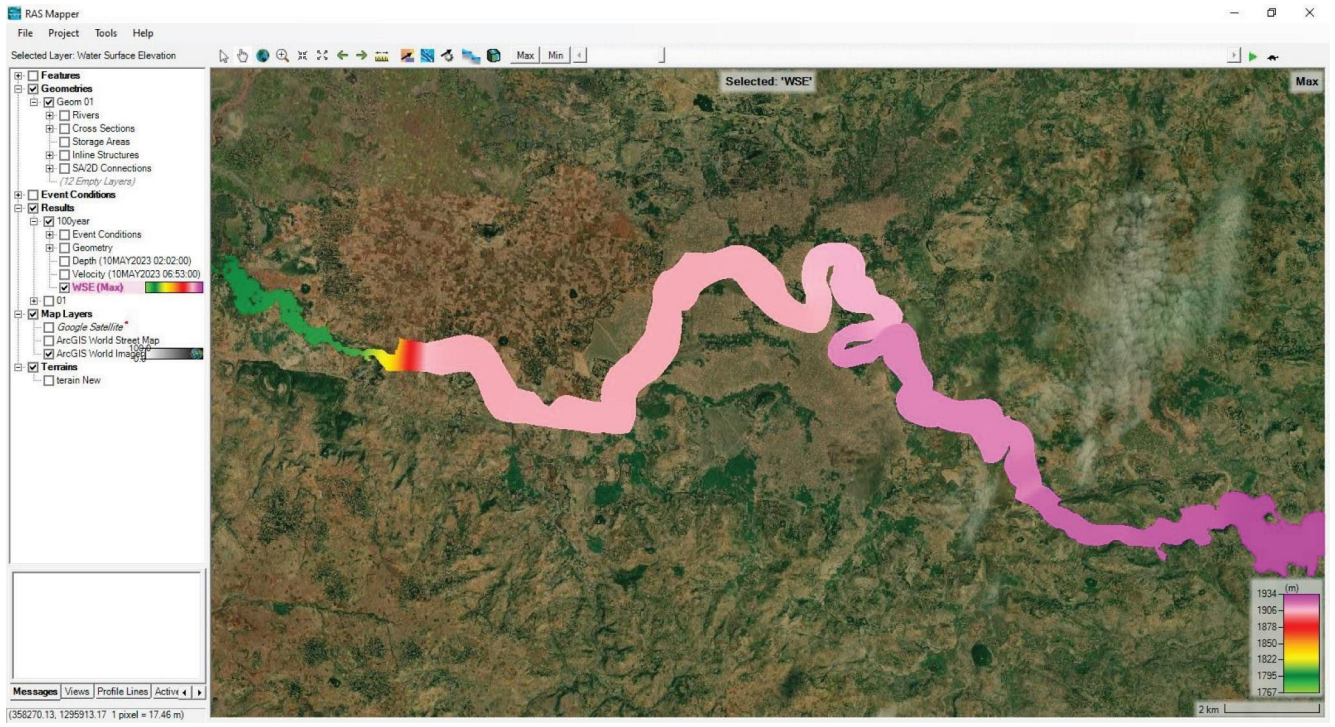

(c)

Figure 9: (a) Flood depth, (b) flood velocity, and (c) water surface.

divert the flow of the river have also been affected by the flood, compromising their functionality and adding to the complexity of managing the floodwaters.

Beyond this general statement, a site-specific measure is very important to avoid the vulnerability of the dam from failure. The first and most important is structural upgrades such as strengthening the spillway or increasing the height of the dam can help to reduce the risk of failure. Since it is a zoned earthen dam, increasing the width and height of the zoned section can reduce the erosion of the downstream section which is seep from the dam. Also, to control the seepage through embankments and pipings due to the flow through the foundation, provide chimney drain combined with horizontal drainage filters.

The other mitigation measures to reduce the dam from failure is sediment management. As shown in the result, the dam will be failed due to overtopping. This over topping of the dam may be due to the capacity of the spillway and the reduction of the reservoir storage due to high sediment inflow to the reservoir. So, to reduce the inflow of the sediment into the reservoir, we recommend sediment management structures in the watershed like reforestation, terracing, and removing the sediment accumulation in the reservoir area.

4. Conclusion

The severity level of a dam breach depends on the size of reservoir, the incoming flood, the method implied to forecast breach, and the settlement magnitude and types on the downstream reaches. The purpose of this study is dam breach modeling and downstream flood mapping for Gumara proposed embankment dam. During an analysis of dam breach hydraulic model, HEC RAS was used. PMF is used in hydraulic model HEC-RAS in unsteady flow as input data. Von Thun and Gillette regression equation was selected to estimate the breach parameter since it was in the reasonable value of breach width, breach development time, and peak discharge based on international limit value for both overtopping and piping failure scenarios.

The estimated breach bottom width is 113 m, side slope 0.5H : 1V, and breach development time is 0.85 hr for overtopping and bottom width is 111 m, side slope 0.5H : 1V, and breach development time is 0.83 hr for pipping. During analysis of flood routing, the peak discharge at the dam site is 19,753.68 m^3/s occurred at 4 hr for overtopping and 25,128.1 m^3/s at time to peak 4 hr for pipping. The peak flood discharge resulted from dam break by pipping mode of failure is greater than by 21.4% that of overtopping mode of failure. So, we conclude that the dam break by pipping mode of failure will develop more risk than overtopping mode of failure. After routing the peak outflow, flow inundation mapping of water depth, water surface extent, and velocity is performed by HEC-GeoRAS in the GIS window. The flood depth after the breach was 15 m. The velocity of the flood was 15 m/s. From the downstream inundated critical location which have problems, one is found on both sides of the river, there is high traditional small-scale irrigation which is inundated by the flood. And also, downstream of the dam, there are villages inhabitate on the sides of the river.

Data Availability

The DEM that supports the findings of this study is available at https://earthexplorer.usgs.gov. The remaining data that support the findings of this study are not openly available and are obtained from corresponding organizations upon reasonable request forms.

Ethical Approval

The submitted work is original and not have been published elsewhere in any form or language (partially or in full).

Conflicts of Interest

The authors declare that they have no conflicts of interest.

Authors' Contributions

Amdeselassie Fikre and Alene Moshe done the study's conception, design, and wrote the first draft of the manuscript. Material preparation, data collection, and analysis were performed by Manamno Beza. All authors read and approved the final manuscript.

References

[1] A. Bharath, A. V. Shivapur, C. G. Hiremath, and R. Maddamsetty, "Dam break analysis using HEC-RAS and HEC-GeoRAS: a case study of Hidkal dam, Karnataka state, India," *Environmental Challenges*, vol. 5, Article ID 100401, 2021.

[2] J. O. Alabi, J. E. Sanni, M. A. Ashiru, M. J. Yusuf, and A. S. Adeoye, "Simulating the failure of doma dam using a mathematical model," *Global Scientific*, vol. 8, no. 75, pp. 147–154, 2020.

[3] J. A. Charles, T. Paul, and W. Allen, "Lessons from historical dam incidents," 2011.

[4] FEMA, *Dam Safety An Owner's Guidance Manual.Pdf*, Colorado Division of Disaster Emergency Services, Colorado, 1987.

[5] FEMA, "Federal guidelines for dam safety," 2004.

[6] T. L. Wahl, *The Uncertainty of Embankment Dam Breach Parameter Predictions Based on Dam Failure Case Studies*, USDA/FEMA Workshop on Issues, Resolutions, and Research Needs Related to Dam Failure Analysis, Oklahoma, 2001.

[7] W.-F. Chen and L. Duan, "Substructure design," 2003.

[8] Y. Xiong, "A dam break analysis using HEC-RAS," *Journal of Water Resource and Protection*, vol. 3, no. 6, pp. 370–379, 2011.

[9] Via, The Charles E and T. A Atallah, "Report a review on dams and breach prepared by: Dr. Muhammad Hajj (Co Chair)," 2002.

[10] M. W. McCann, "Dam failures in the U.S," *National Performance of Dams Program*, pp. 0–10, 2018.

[11] T. L. Wahl, "Prediction of embankment dam breach parameters—a literature review and needs assesment," *Water Resources Research*, vol. 67, 1998.

[12] J. E. Costa, "Floods from dam failures," in *U.S. Geological Survey Open-File Rep*, U.S. Geological Survey Denver, Colorado, 1985.

[13] P. W. Rkahawita, "Modeling the hydraulics and erosion process in breach formanon due to overtopping," *Sedimentation AndSediment Transport*, pp. 211–220, 2002.

[14] V. P. Singh and P. D. Scarlatos, "Analysis of gradual earth-dam failure," *Journal of Hydraulic Engineering*, vol. 114, no. 1, pp. 21–42, 1988.

[15] T. L. Wahl, "Dam breach modeling-an overview of analysis methods," in *In 2nd Joint Federal Interagency Conference*, Las Vegas, 2010.

[16] T. J. R. Hepler and E. Thomas, "Innovative dam and levee design and construction for sustainable water management," in *32nd Annual USSD Conference*, p. 222, United States Society on Dams, New Orleans, Louisiana, 2012.

[17] C. Chinnarasri, S. Jirakitlerd, and S. Wongwises, "Embankment dam breach and its outflow characteristics," *Civil Engineering and Environmental Systems*, vol. 21, no. 4, pp. 247–264, 2004.

[18] H. P. Fernandes, *Analysis of dam failures and development of a dam safety evaluation program*, Thesis, Ohio State University, 2014.

[19] H. H. Mhmood, M. Yilmaz, and S. O. Sulaiman, "Simulation of the flood wave caused by hypothetical failure of the Haditha dam," *Journal of Applied Water Engineering and Research*, vol. 11, no. 1, pp. 66–76, 2023.

[20] FEMA, *Federal Guidelines for Inundation Mapping of Flood Risks Associated with Dam Incidents and Failures*, FEMA, 1st edition, 2013.

[21] V. Nourani and S. Mousavi, "Evaluation of earthen dam-breach parameters and resulting flood routing case study: aidoghmosh dam," *International Journal of Agriculture Innovations and Research*, vol. 1, no. 4, pp. 109–115, 2013.

[22] S. K. Garg, *Irriagtion Engineering & Hydraulic Structures*, Khanna Publishers, New Delhi, 2005.

[23] P. Novak, *Developments in Hydraulic Engineering-5*, Elsevier Applied Science Publishers LTD, UK, 2005.

[24] Arkansas Natural Resources Commission, *Dam Safety Guidance Manual*, Arkansas Natural Resources Commission, 2022.

[25] R. B. Jansen, "Advanced Dam Engineering For Design, Construction, and Rehabilation," Springer, New York., 1988.

[26] WWDSE, *Gumara Irrigation Project Dam & Appurtenant Works*, WWDSE, Addis Ababa, Ethiopia, 2008.

[27] J. Chamberlin and E. Schmidt, "Ethiopian agriculture: a dynamic geographic perspective," in *Food and Agriculture in Ethiopia: Progress and Policy Challenges*, P. Dorosh and S. Rashid, Eds., pp. 21–52, University of Pennsylvania Press, Philadelphia, 2013.

[28] H. Lemma and S. Demissie, "Climate change impact assessment on water resources of gumara watershed, upper blue nile river basin," *Journal of the American Chemical Society*, vol. 123, no. 10, pp. 2176–2181, 2013.

[29] M. A. Wubneh, F. T. Fikadie, T. A. Worku, T. F. Aman, and M. S. Kifelew, "Hydrological impacts of climate change in gauged sub-watersheds of Lake Tana sub-basin (Gilgel Abay, Gumara, Megech, and Ribb) watersheds, Upper Blue Nile Basin, Ethiopia," *Sustainable Water Resources Management*, vol. 8, no. 3, pp. 1–14, 2022.

[30] D. Michael Gee, "Comparison of dam breach parameter estimators," in *World Environmental and Water Resources Congress 2009*, pp. 1–10, ASCE Library, 2009.

[31] A. Leoul and N. Kassahun, "Dam breach analysis using HEC-RAS and HEC-GeoRAS: the case of Kesem Kebena dam," *Open Journal of Modern Hydrology*, vol. 9, no. 4, pp. 113–142, 2019.

[32] J. N. Duressa and A. K. Jubir, "Dam break analysis and inundation mapping, case study of fincha'a dam in horro

guduru wollega zone, oromia region, Ethiopia," *Science Research*, vol. 6, no. 2, pp. 29–38, 2018.

[33] D. C. Froehlich, "Embankment dam breach parameters and their uncertainties," *Journal of Hydraulic Engineering*, vol. 134, no. 12, pp. 1708–1721, 2008.

[34] T. C. MacDonald and J. Langridge-Monopolis, "Breaching charateristics of dam failures," *Journal of Hydraulic Engineering*, vol. 110, no. 5, pp. 567–586, 1984.

[35] L. J. V. Thun and D. R. Gillette, *Guidance on Breach Parameters*, Internal Memorandum, U.S. Dept. of the Interior, Bureau of Reclamation, 1990.

[36] U.S. Bureau of Reclamation, "Downstream hazard classification-guidelines," in *ACER Technical Memorandum No. 11*, Denver, 1988.

[37] D. C. Froehlich, "Embankment dam breach parameters revisited," in *Proceeding 1st International Conference on Water Resources Engineering*in *American Society of Civil Engineers*, pp. 887–891, New York, 1995.

[38] L. Hayimanot, *Dam breach modelling and downstream risk analysis using (For Arjo-Dedessa Dam)*, Unpublished Master's thesis, Addis Ababa University, 2015.

[39] HEC, *HEC-GeoRAS GIS Tools for Support of HEC-RAS Using ArcGIS ® User's Manual*, US Army Corps of Engineers Institute for Water Resources Hydrologic Engineering Center, 2005.

[40] V. T. Chow, *Open Channel Hydraulics. McGraw-Hill*, McGraw-Hill, New York, 1959.